Computational and Structural Biotechnology Journal 28 (2025) 50–62

Contents lists available at ScienceDirect

Computational and Structural Biotechnology Journal

journal homepage: www.elsevier.com/locate/csbj

Research article

Lateral walking gait phase recognition for hip exoskeleton by denoising autoencoder-LSTM

Mingxiang Luo [a], Xiaoli Dong [b], Hongliu Yu [c], Mingming Zhang [d], Xinyu Wu [a], Worawarit Kobsiriphat [e], Jing-Xin Wang [f], Wujing Cao [a,*]

[a] Guangdong Provincial Key Lab of Robotics and Intelligent System, Shenzhen Institute of Advanced Technology, Chinese Academy of Sciences, Shenzhen 518005, China
[b] Xinjiang Industrial Vocational and Technical College, Urumqi 830000, China
[c] University of Shanghai for Science and Technology, Shanghai 200093, China
[d] Southern University of Science and Technology, Shenzhen 518055, China
[e] The National Metal and Materials Technology Center, Pathum Thani 12140, Thailand
[f] Department of Rehabilitation, Zhengzhou Central Hospital Affiliated to Zhengzhou University, Zhengzhou 450000, China

ARTICLE INFO

Keywords:
Lateral walking gait recognition
Hip exoskeleton
DAE-LSTM
IMUs

ABSTRACT

Lateral resistance walk is an effective way to strengthen the abductor muscles of the hip. Accurate lateral walking gait recognition is the prerequisite for exoskeletons to be applied to lateral walking exercises. This paper proposes a denoising autoencoder-LSTM (DAE-LSTM) algorithm for lateral walking gait recognition. Nine sets of IMU data at three speeds and three strides of ten subjects were collected. Four lateral walking gait phases of narrow double support (NDS), guided foot swing (GFS), wide double support (WDS) and following leg swing (FLS) were recognized. The recognition performance of random forest (RF), support vector machine (SVM), k-nearest neighbors (KNN), neural networks (NN) and DAE-LSTM were compared. The average cross-subject recognition accuracy of DAE-LSTM was 90.2 %, which was higher than the other four models and previous work. For each frame of IMU data, the average recognition time of DAE-LSTM is 0.383 ms, which is 5.32 ms higher than the previous work. When the signal-to-noise ratio (SNR) is greater than 100:1, the accuracy of the DAE-LSTM model is higher than 90.0 %, and the accuracy of the other four models were less than 85 %. The results show that the proposed algorithm can achieve the requirements of recognition accuracy, model recognition time and model robustness for application in exoskeleton.

1. Introduction

Hip abductor muscle plays a key role in controlling pelvic stability, alleviating knee pressure and maintaining the balance of lower limb force lines. The adductor muscle of the hip is also important in maintaining the symmetry and coordination of the body's dynamics. Weakness and reduced activity of the adductor and abductor muscles of the hip often lead to abnormal gait, which increases the risk of falls, especially in the elderly or in patients recovering from lower limb injuries. Therefore, it is necessary to strengthen the adductor and abductor muscles of the hip joint through rehabilitation training [1]. As an effective way to strengthen the hip abductor muscle, lateral resistance walking can not only improve muscle strength, but also promote the flexibility and stability of the hip joint, which is essential for maintaining balance and stability during movement [2]. As shown in Fig. 1(a), traditional abductor muscle training methods are achieved by wearing resistance bands on the lower extremities. However, this method has significant limitations: 1. Unable to provide stable resistance torque, resulting in low training accuracy and unsatisfactory effect. 2. The freedom of forward walking will be limited, and more complex gait training cannot be realized. 3. This method does not strengthen the adductor muscle of the hip joint. 4. Due to the lack of sensors and actuators, the method cannot evaluate and adjust the exercise intensity in real time according to the state of the wearer.

Wearable exoskeletons have been widely used in walking assistance. The exoskeleton may provide resistance instead of assistance to be applied to lateral resistance walk. In order to deal with problems existing in lateral band walk, our team designed a hip exoskeleton to provide resistance during lateral walking gait, as shown in Fig. 1(b). For different patients, the output resistance of the exoskeleton can be intelligently

* Correspondence to: Shenzhen Institute of Advanced Technology Chinese Academy of Sciences, China.
E-mail address: caowujing414@126.com (W. Cao).

https://doi.org/10.1016/j.csbj.2025.02.001
Received 14 August 2024; Received in revised form 2 February 2025; Accepted 2 February 2025
Available online 5 February 2025

controlled to meet the personalized exercise needs. The lateral walking gait phase recognition is the premise of exoskeleton control. Therefore, it is important to research algorithm which can accurately identify the lateral walking gait phase.

The sensors used have direct effect on the signal acquirement and recognition accuracy. A few of researchers have researched various gait detection algorithms based on different wearable sensors. Morbidoni et al. studied machine-learning-based approach to binary classify gait events by sEMG signals in hemiplegic-child walking [3]. However, due to sweating and fatigue during human movement, the accuracy of intent recognition based on EMG signals decreases over time. Wei et al. combined features extracted from sEMG and EEG channels for gait phase recognition to study the recognition effectiveness of different neural networks [4]. However, the complexity of signal processing in EEG is an important issue. At the same time, wearing myoelectric devices for long time is inconvenient for users.

Recently, the application of inertial measurement unit (IMU) has brought more and more attention for gait recognition. IMU is easy to wear, small size and has high tolerance to the environment. A few of exploration have been conducted for gait detection of lower limb exoskeletons and prosthetics based on IMU. In [27], the authors use wearable sensing technology with an inertial measurement Unit (imu) to enable portable and customized gait retraining for knee osteoarthritis. Guo et al. proposed a new method called Online gait phase prediction (OGPP) based on IMU signals and used pseudo-tags for gait phase prediction [28]. Chen et al. introduce a method for real-time recognition of gait events using IMU. The experimental results show that the proposed method achieves good results in the identification of early feature points of initial contact (IC) and toe-off (TO) events [29]. Liu et al. proposed a lower limb IMU signal method based on fuzzy logic to identify events when the heel and toe contact or leave the ground [30]. Cheng et al. proposed an activity recognition system that uses signals from a thigh-mounted IMU and a force sensitive resistor to classify transitions between sitting, walking, stair ascending, and stair descending [5]. Bartlett et al. presented a gait classification method based on phase variable description by measured motion of the thigh segment provided by an inertial measurement unit [6]. Su et al. proposed a method for processing IMU signals based on CNNs, and the recognition accuracy of 13 types of motion intentions reached a high level [7]. Chen et al. proposed a foot position prediction method based on Bayesian inference for wearable IMU sensors to predict foot position in the early swing phase [8]. Above studies aimed at the gait under forward walking.

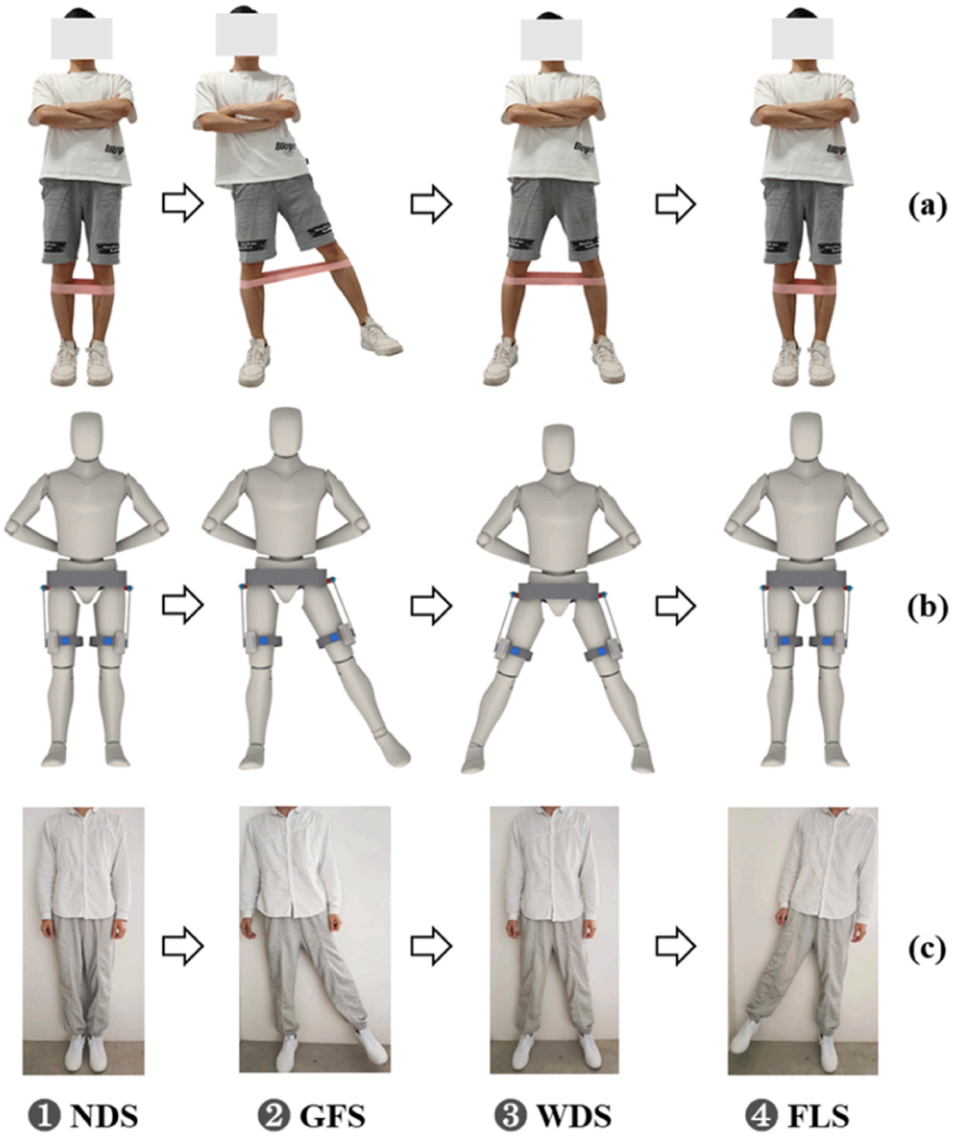

Fig. 1. Lateral walking with hip resistance exoskeleton to replace elastic band. (a) Lateral walking with elastic resistance band. (b) Lateral walking with hip resistance exoskeleton. (c) The complete lateral walking gait cycle.

Although the lateral walking gait is completely different from the forward walking, they play a good role for reference of the IMU-based lateral walking gait detection.

For the recognition of lateral walking gait with fixed stride length, our team previously conducted a preliminary exploration using traditional existing algorithms [9]. However, due to differences in the stride length and speed of different groups of people, our previous exploration had certain limitations. A gait recognition method for lateral walking which is suitable for various stride lengths and speeds needs to be studied. As far as we know, the algorithm developed for lateral walking gait recognition is almost blank. However, the algorithms used in forward walking can be referred. In [10], the authors extracted the time-domain features of IMUs and predicted motion patterns through linear discriminant analysis (LDA). Ryu et al. identified four gait phases based on the support vector machine (SVM) and achieved good recognition accuracy [11]. Compared to other machine learning methods, deep learning is more capable of finding deep connections between features and labels. In [12], the authors designed a variety of different deep neural networks to predict the subject's motion pattern and transition intention in real time only through the data of IMU. Based on the influence of muscles on the classification of gait phases, Wei et al. identified the gait phases by long short-term memory (LSTM) and achieved good recognition results [13]. Luo et al. combined LSTM with multilayer perceptron (MLP) for predicting gait subphases and the recognition accuracy was superior to other existing methods [14]. Similar to forward walking, the lateral walking gait phase changes periodically. In other words, the time-dependent performance of the lateral walking gait phase has greater benefits for gait recognition. For these reasons, we use long short-term memory (LSTM) to design a transverse gait phase classifier.

IMUs are usually connect to a computer via Bluetooth technology. Thus, IMU signals often include noise due to the impact of the environment. The use of noise-reducing autoencoders can improve data quality to some extent. Autoencoders are often used to reconstruct new feature data from the original data. Jun et al. proposed a method to extract features using two RNN autoencoders, which improved the recognition accuracy of abnormal gait recognition [15]. Tu et al. designed a spatiotemporal data augmentation method based on LSTM autoencoder network and applied it to the bone-based human motion recognition [16]. Zhang et al. proposed an autoencoder framework to clarify the relationship between confounding features to improve the accuracy of gait recognition [17]. Sheng et al. proposed a conjoined noise reduction autoencoder for joint trajectory reconstruction and robust gait recognition [18]. Wang et al. proposed a stride estimation method based on LSTM and denoising autoencoder (DAE) to solve the error caused by the estimation of the motion distance of natural walking under complex conditions [19]. Noise-reducing autoencoders reduce the effect of noise disturbances in signals by adding noise to the signal and then reconstruct it. In order to make the designed lateral walking gait recognition algorithm more robust and meet the needs of multiple types of people. In this paper, a noise reduction encoder is used to design a lateral walking gait phase classifier to overcome the interference of IMU signals.

The main contributions of this work are as follows:

(1) Based on IMU signals, this paper proposed a noise reduction autoencoder and LSTM fusion method (DAE-LSTM) for lateral walking gait recognition. The lateral walking gait with three stride lengths and three speeds is studied for the first time. Four lateral walking gait phases including narrow double support (NDS), guide foot swing (GFS), wide double support (WDS), and following leg swing (FLS) were identified based on the proposed algorithm.
(2) Compared with the performance of four algorithm models RF, SVM, KNN, and NN, the proposed DAE-LSTM model achieves better recognition result during cross-subject experiments. In addition, compared with previous studies with fixed stride length, the proposed model has better cross-subject recognition accuracy and greater recognition time performance.
(3) For signals with different signal-to-noise ratios, the noise immunity of the five algorithm models was compared experimentally. Compared with the other four models, the proposed DAE-LSTM has stronger robustness.

2. Methods

2.1. Gait division

Similar to the forward walking gait, the lateral walking pattern requires a defined direction. In this study, the rightward movement relative to the human body serves as the designated travel direction, whereas movement towards the left side constitutes the retracing direction. When proceeding in the forward direction, the right leg functions as the guide leg, while the left leg acts as the following leg. Our focus pertains to lateral walking in the forward direction. Illustrated in Fig. 1(c), a complete lateral walking gait cycle is established for this study. The first gait phase is defined as narrow double support (NDS). At this phase, the human body stands vertically on flat ground. There is almost no distance between the legs of the human body. The second phase of gait is defined as guided foot swing (GFS). At this phase, as the front legs are off the ground, the weight of the body is gradually transferred to the back legs. When the front leg hits the ground, it is defined as the end of the second phase. The third phase of gait is defined as wide double support (WDS). At this phase, the human body stands on flat ground with both legs. The human legs are separated by a certain distance, and the center of gravity gradually shifts between the legs. The fourth phase of gait is defined as following leg swing (FLS). At this phase, as the hind legs leave the ground, the weight of the body gradually shifts to the front legs. The moment the hind leg hits the ground is defined as the end of the fourth phase of the gait.

In this study, the plantar pressure sensor's acquired signal serves as a pivotal indicator for gait phase recognition. Based on the plantar pressure signal, we divide the IMU signal into four phases of gait. Based on the plantar pressure signal, we divide the IMU signal into four gait phases. During the model training process, the signal obtained from the plantar pressure sensor is employed as the actual class. The IMU signal recognized by the model is employed as the predicted class.

2.2. Structure and prototype

Based on the design requirements and the function of the biomechanical analysis, our team designed a hip exoskeleton and its structure is shown in Fig. 2(a). The width adjustment class has a range of 200 mm and can be adjusted to suit different body types.

Fig. 2(a) also shows a side view of the wearer. The exoskeleton is connected to the wearer by a lumbar support, a rigid cowhide belt in the prototype. Four pressure gasket modules (FSR, Kcut, China) are placed at the first metatarsal and posterior heel of the forefoot to detect the lateral walking gait phase. Two IMUs (LPMS-B2, Arubi, China) are attached to the thigh brace in front of the thigh, to measure attitude information when walking.

2.3. Signal acquisition

This study collected IMU signals from 9 channels as raw data: 3 tilt angles (roll, pitch, and yaw) and angular velocities and linear accelerations on the X, Y, and Z axes. The system architecture is shown in Fig. 2 (b). The attitude signals of the IMU are sent to the single-chip microcomputer through Bluetooth technology. Select the IMU sampling rate based on actual application requirements, application scenarios, and device performance. If the collected data needs to be processed in real time or is a complex dynamic motion, a higher sampling rate is required

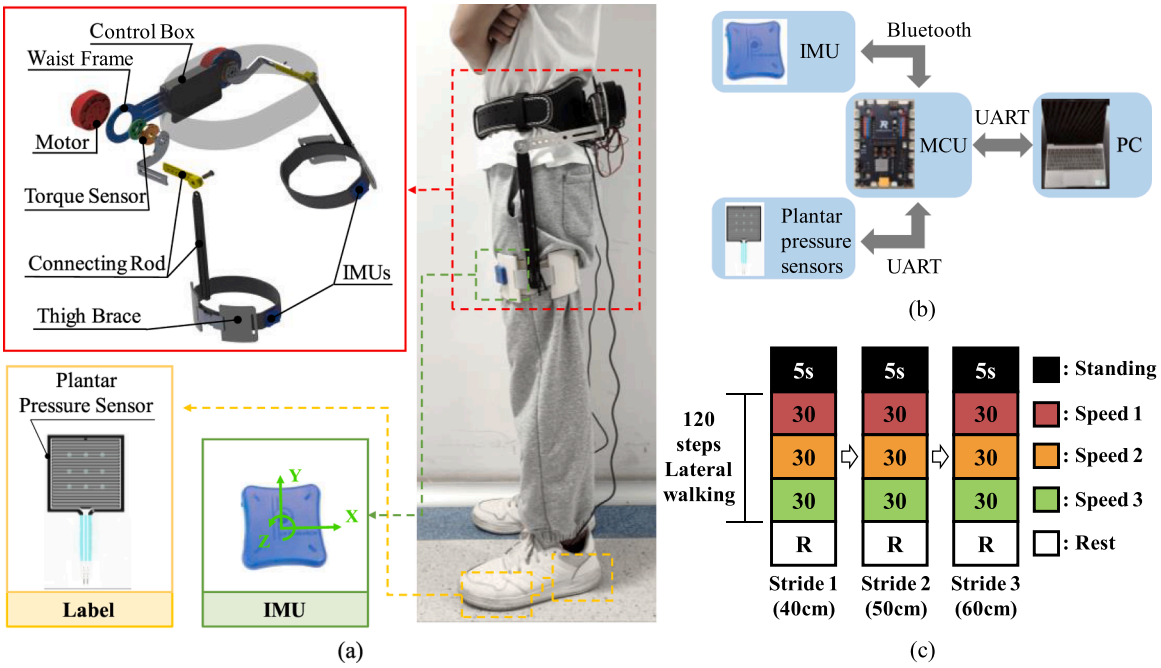

Fig. 2. Lateral resistance exoskeleton experimental equipment, system architecture and experimental protocol. (a) Lateral resistance exoskeleton experimental equipment. The hip exoskeleton was worn on the subject, and the IMU and plantar pressure sensors were attached to record changes in biological signals during the experiment (b) The system architecture. The hardware includes an IMU, plantar pressure sensors, an MCU and PC. (c) The experimental protocol. Each subject was asked to walk laterally in three sets of strides, each consisting of three speeds. And each speed requires 30 steps. Each group began by standing for five seconds. Then walk 30 steps according to the three speeds from fast to slow. Finally, they entered the rest phase, where participants were asked to rest for 3 minutes.

in order to capture key signal changes. If it is used for offline analysis or low speed steady motion, a lower sampling rate can be selected. High sampling rates increase data volume and power consumption, challenging the portability and battery life of the exoskeleton. In this paper, the signal acquisition frequency of IMU is 200 Hz. The IMU is placed above the knee joint to effectively capture the biomechanical properties of the lateral gait. Plantar pressure sensors are placed on the forefoot and back heel of the soles of both feet. The plantar pressure signals of the pressure sensor are sent to the microcontroller via a universal asynchronous transceiver (UART). The plantar pressure signal is acquired at a frequency of 200 Hz. In addition, synchronization with plantar pressure or other signals is also a key issue when IMU signals are applied to exoskeleton systems. In this paper, the single-chip microcomputer was used to synchronously collect the attitude signal and plantar pressure signal of the experimental subject during the experiment in real time. Then, the synchronized attitude signal and plantar pressure signal are sent to the PC through the UART.

A total of 10 subjects were recruited for this study. The study was approved by the Medical Ethics Committee of Shenzhen Institute of Advanced Technology (SIAT-IRB-200715-H0512). In the in-subject experiment, the collected IMU data and plantar pressure signals are used to create the experimental data set. Fig. 3 shows the process of model training and recognition.

Before the start of the experiment, we explained the experimental process in detail to all subjects and conducted pre-experiments. Each subject was asked to perform three sets of lateral walking experiments with unsynchronized amplitudes. The experimental protocol is shown in Fig. 2(c). Each set of lateral walking experiments was defined as walking 30 steps sideways along a straight line. In each experiment, subjects were asked to walk laterally at three different speeds. Among them, three stride lengths were selected as 40 cm, 50 cm, and 60 cm. Three speeds were selected as 1.87 sec/step, 1.67 sec/step and 1.46 sec/step. When the stride length is 40 cm, the corresponding speeds of the three speed modes are 21.3 cm/s, 24.0 cm/s, and 27.4 cm/s, respectively.

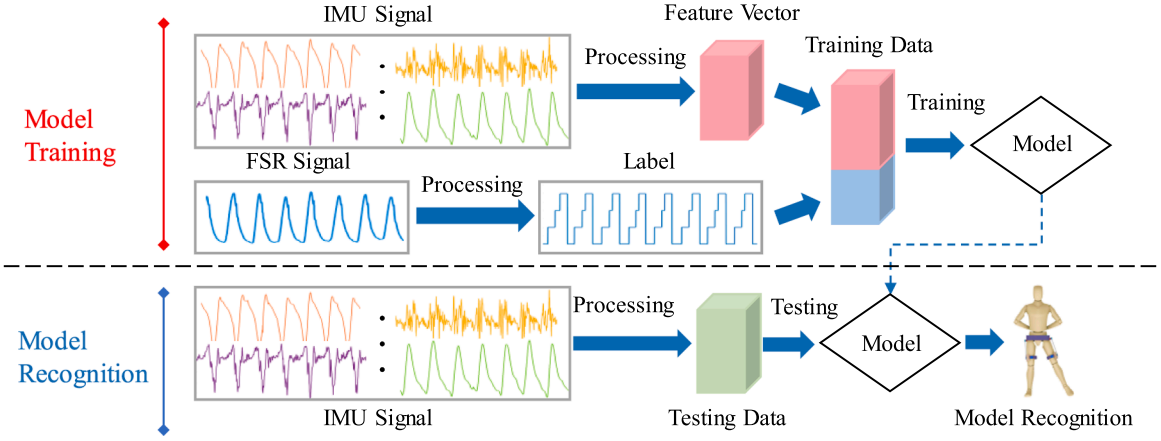

Fig. 3. The process of model training and recognition across subjects.

When the stride length is 50 cm, the corresponding speeds of the three speed modes are 26.5 cm/s, 29.8 cm/s, and 34.0 cm/s, respectively. When the stride length is 60 cm, the corresponding speeds of the three speed modes are 31.9 cm/s, 35.9 cm/s and 40.8 cm/s, respectively. At the end of each experiment, the subjects were asked to return to the origin point to rest for 3 minutes and prepare for the next set of experiments. In order to ensure that the stride length of each step in the same set of experiments is the same, we intervene by marking the experimental site. In order to ensure that the speed of lateral walking of subjects in the same group of experiments is consistent, we use metronome to respond in a certain time interval to control it. The entire experimental procedure was carried out on the flat ground. The experiment collected a total of 2700 steps of data. After we checked and screened out some seriously damaged data, a total of 2479 steps of data were finally used for subsequent model training and testing.

2.4. Signal preprocessing

In this study, the acquired IMU signals are filtered by the sensor's own Kalman filter. Kalman filtering dynamically reduces noise caused by sensor drift and environmental interference, effectively suppressing both high- and low-frequency noise to ensure smoother and more stable signals. It also enhances data consistency by optimizing multivariate state estimation, improving the quality of time-series features for the model. By minimizing random noise, Kalman filtering allows the model to focus on key gait features, such as acceleration and angular velocity, thereby enhancing recognition accuracy and robustness. Fig. 4 shows the 6 channel IMU signals in one gait cycle after filtering, including the Angle, angular velocity and linear acceleration of x and z axes. Each channel displays 9 types of signals with 3 stride lengths and 3 speeds. Then, the resulting feature vectors are normalized. Finally, a 6-dimensional feature vector (including six IMU channels) is formed.

2.5. Algorithmic models

The classifier is related to the effect of gait recognition. At present, it is difficult to find papers on lateral gait recognition based on IMU signals. To this end, we conduct experimental evaluation of the current model with strong versatility. These algorithmic models include: Random Forest (RF), Support Vector Machine (SVM), K-Nearest Neighbors (KNN), Neural Networks (NN). The IMU signal is a time series signal. For different wearers, the trained classifier is required to have better cross-subject ability. In recent years, the LSTM model has shown good recognition effect on time series signals. Based on above reasons, the author proposes a noise reduction encoder and LSTM fusion algorithm to compare with above four algorithms. A 10x cross-validation strategy was adopted. Then, different parameter settings were tested for each algorithm model.

1) Random Forest: RF is a commonly used classification algorithm. Its basic unit is the decision tree. Its output category is determined by the voting results of multiple decision tree. Compared to decision trees, it effectively reduces overfitting and results in better performance. The splitting criterion is Gini impurity and the feature selection is log2 scaling.
2) Support Vector Machine: SVM is a machine learning algorithm that is often used for binary classification. Its basic idea is to find a dividing hyperplane in sample space. This hyperplane separates different classes of samples while maximizing the distance from the edge points in the set of two points to this plane. The equation for the hyperplane is as follows:

$$w^T x + b = 0$$

where x is the input feature (i.e. feature vector), w is the weight vector, b is the bias. The weight vector determines the direction of the hyperplane, while the bias determines its position. In this paper, the SVM model uses RBF kernel function, kernel parameter gamma = 0.01, regularization parameter C = 1.0.
3) K-Nearest Neighbors: First, given a trained sample set, for the new input sample, find K samples closest to the sample in the training sample set, and most of these K samples belong to a certain category, and the input sample is classified under this category. For this algorithm, there are three important factors to consider. The first is the selection of distance, and Euclidean distance is chosen as the measurement. This is followed by the selection of K -values, which in this study we chose as 8. The final step is the choice of decision-making method. The method of voting for the majority was used. And use the method of 10 fold cross verification. For the selected K -value and distance, the new sample belongs to the larger class of samples in this range.
4) Neural Networks: A typical NN mainly consists of input layers, hidden layers, and output layers. For the purposes of this study, neural networks were chosen to solve classification problems. Its main principle is to continuously update the network parameter weights by selecting a certain optimization algorithm according to the input feature vectors and labels, and finally make the output category of the model constantly close to the real category. The neural network model used in this study consists of one input layer, two hidden layers, and one output layer. The learning rate is set to 0.001. Use the Adam optimizer for training. The batch size and epoch are 16 and 70,

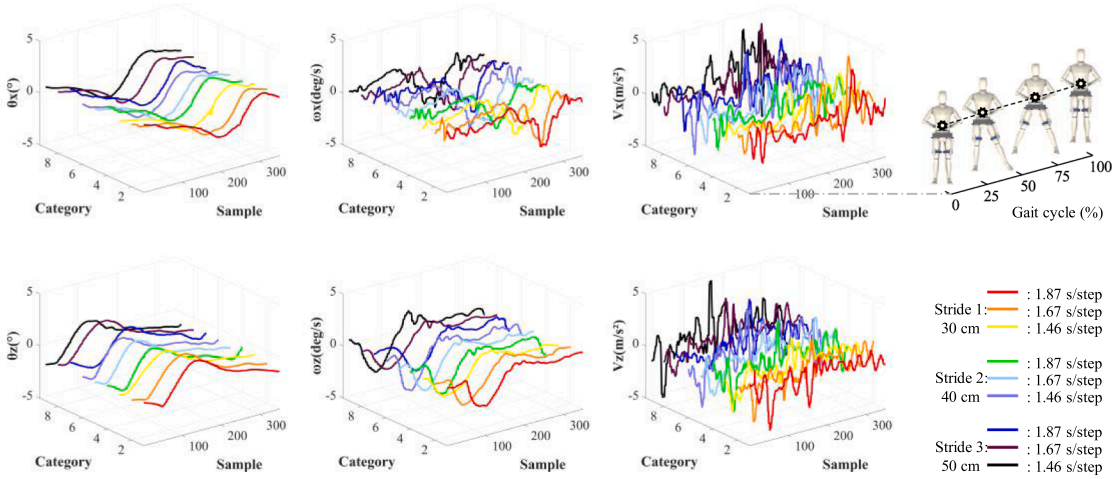

Fig. 4. Six channel IMU signals in one gait cycle after filtering.

respectively. The Softmax function was selected as the activation function of the network output layer. The formula is as follows:

$$S(z)_i = \frac{e^{z_i}}{\sum_{j=1}^{J} e^{z_j}}$$

where $S(z)_i$ is the activation value of one input of the neuron, and z_i and z_j are the elements of the input of the neuron. In this study, the output of the model is four different gait phases. For multi-classification problems, this study uses multi-class cross-entropy loss as the loss function. The formula for the multiclass cross-entropy loss function is as follows:

$$Loss = -\frac{1}{n}\sum_{i=1}^{n}\sum_{j=1}^{m} y_{ij}\log\widehat{y}_{ij}$$

where n is the number of samples input by the model, m is the number of classes output by the model, y_{ij} represents the true value of the jth category of the ith sample, and $\widehat{y}_{ij}$ represents the predicted value of the jth category of the ith sample. The gradient descent method is selected in the backpropagation process of the model. Each input z needs to be derived during backpropagation. The derivation formula is as follows:

$$\frac{\partial Loss}{\partial z} = \widehat{y}_{ij} - y_{ij}$$

5) Long Short-Term Memory: LSTM is a kind of recurrent neural network (RNN) which is especially suitable for processing time series data. It can effectively process and remember the temporal dynamics of the information, so that the model can take into account the temporal and historical information of the signal. Each LSTM cell contains three main gates: the forget gate, the input gate, and the output gate, as well as a memory cell state.The forget gate determines how much information needs to be retained in the memory unit state C_{t-1} of the previous time step. Its calculation formula is as follows:

$$f_t = \rho\left(G_f \bullet [h_{t-1}, x_t] + a_f\right)$$

Where G_f is the weight matrix. a_f is the bias vector. ρ is the Sigmoid activation function. h_{t-1} is the hidden state of the previous time step. x_t is the input to the current time step. The input gate determines how much information in input x_t of the current time step needs to be written to the memory unit. The formula is as follows:

$$i_t = \rho(G_i \bullet [h_{t-1}, x_t] + a_i)$$

Where G_i is the weight matrix. a_i is the bias vector. The candidate memory unit state is generated through the tanh layer to update the memory unit state:

$$\widetilde{C}_t = \tanh(G_c \bullet [h_{t-1}, x_t] + a_c)$$

Where G_c is the weight matrix. a_c is the bias vector. tanh is the tanh activation function. Update the memory unit status by combining the information of the forget gate and the input gate. The output gate determines the output of the current time step. The hidden state of the current time step is calculated using the output gate and the updated memory unit state. The calculation formula is as follows:

$$C_t = f_t \bullet C_{t-1} + i_t \bullet \widetilde{C}_t$$

$$o_t = \rho(G_o \bullet [h_{t-1}, x_t] + a_o)$$

$$h_t = o_t \bullet \tanh(C_t)$$

Where C_{t-1} is the memory unit state of the previous time step. C_t is the memory unit state of the current time step. G_o is the weight matrix. a_o is the bias vector. The LSTM model consists of an input layer, an LSTM layer, a fully connected layer, and an output layer. The Softmax function was selected as activation function of the output layer. The training epoch is 100 and the batch size is 32. The Adam optimizer was used to train the model.

6) Denoising Autoencoder-LSTM: The LSTM model is an algorithm commonly used to process time series signals and have been applied to gait recognition [20]. In this study, the trained classifier in intended to be used on exoskeletons for online real-time recognition of lateral walking. For different wearers, the trained classifier is required to have excellent cross-subject ability. Inspired by the good performance of LSTM in gesture and gait recognition [21–23]. In order to enhance the robustness of the classifier, we proposed an algorithm for the fusion of noise reduction autoencoder and LSTM to identify the lateral gait phase. The core idea of the noise reduction autoencoder is to add noise to the input sample data to make the data deviate from the actual sample data to a certain extent. This data is then used as the training data for the autoencoder. The autoencoder reconstructs the features of this part of the training data. The purpose of feature reconstruction is to make the data output by the autoencoder as close as possible to the data without added noise. In this study, the data output by the noise-reducing autoencoder is used as input to the LSTM. The Lateral walking gait recognition method framework based on DAE-LSTM model is shown in Fig. 5. The collected biosensor signals of the subjects were preprocessed and then fed into the DAE-LSTM model for recognition. The DAE module consists of an input layer, three hidden layers, and an output layer. L2 weight regularization (0.001) and sparse regularization (4) were applied. The input layer represents the acquired IMU signals. The DAE module adjusts network parameters by minimizing the error between the input and the reconstructed signals. The output layer represents the reconstruction of deep features. The data output by the DAE module is trained as the input of the LSTM module. The LSTM module consists of an input layer, an LSTM layer, a fully connected layer, and an output layer. The Softmax function was selected as activation function of the output layer. The training epoch is 100 and the batch size is 32. The Adam optimizer was used to train the model.

2.6. Performance evaluation

The performance of the lateral walking gait phase recognition system is significant to the exoskeleton system. The recognition accuracy, model recognition time, and model robustness were used to evaluate the performance of the model.

1) Recognition accuracy: Recognition accuracy is an important indicator for evaluating model performance. The recognition accuracy in this study included the in-subject group and the cross-subject group. A confusion matrix is a way of describing recognition accuracy. It is also chosen to evaluate the recognition accuracy in this work. The recognition accuracy for each gait phase is as shown:

$$P_{ij} = \frac{s_{ij}}{s_i} \times 100\%$$

where s_{ij} represents the number of samples that actually belong to gait phase i which are identified as gait phase j. s_i represents the total sample size that actually belongs to gait phase i. P_{ij} represents the percentage of s_{ij} and s_i. The recognition accuracy of all gait phases can be expressed using a confusion matrix, as shown:

$$Y = \frac{\sum_{i=j}^{n} s_{ij}}{S}$$

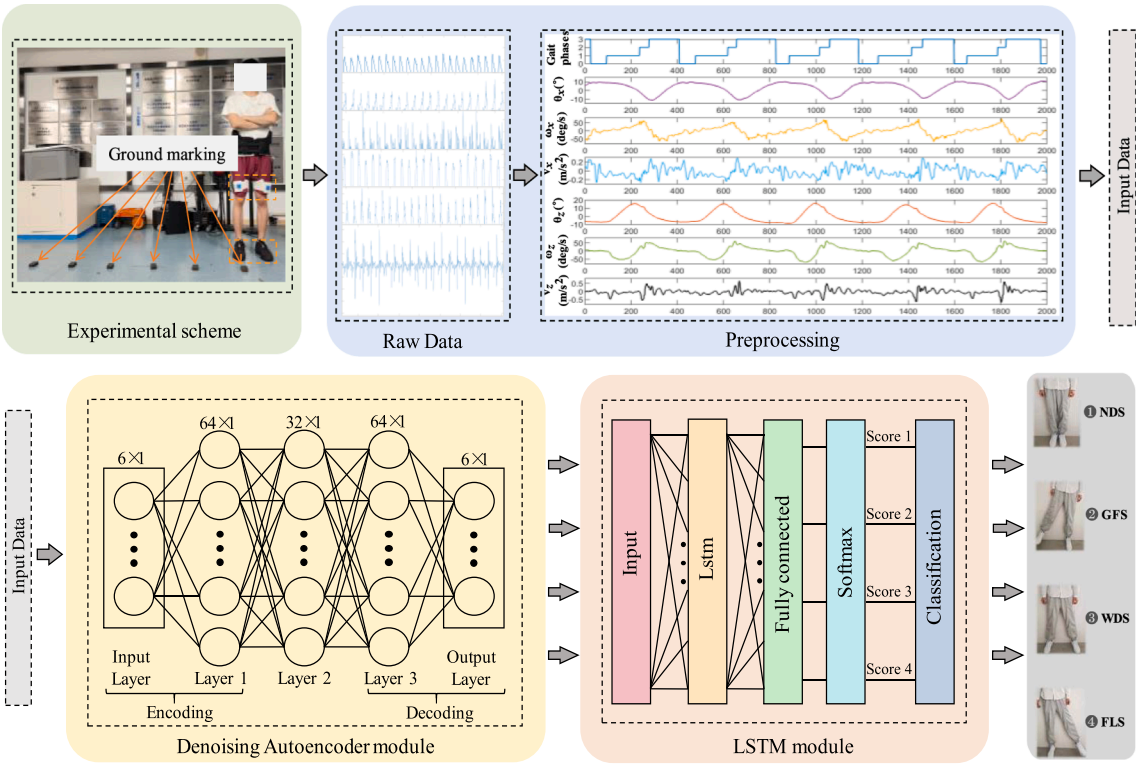

Fig. 5. Lateral walking gait recognition method framework based on DAE-LSTM model.

where n represents the number of gait phases, with a value of 4. S represents the total number of all samples that the method put into the model for testing. When i = j, s_{ij} represents the number of samples that actually belong to the same gait phase and the gait phase that is recognized. Y represents the number of samples that were correctly predicted as a proportion of the total number of all samples, i.e. the total accuracy.

2) Model recognition time: The model recognition time was obtained based on the experimental data gathered from the across-subject group. It includes offline recognition time and real-time recognition time. The IMU signals collected in real time during the experiment were filtered and imported into the model for recognition. The time required for this process is called real-time recognition time. In practical applications of the real-time recognition system, the recognition time holds paramount importance. The difference between offline recognition time and real-time recognition time is that the process of model recognition is carried out offline.
3) Model robustness: For diverse users, the recognition system is required to have good robustness. This means that the recognition system should have good classification capability while IMU signals have a certain amount of noise. The signal-to-noise ratio represents the ratio of the original signal to the added noise. A higher signal-to-noise ratio value means less noise. Conversely, a smaller signal-to-noise ratio value means more noise added. Noise with different signal-to-noise ratios was added to the IMU signals across the subjects. And then different algorithm models were selected for offline recognition and classification. The better the offline recognition performance, the stronger the robustness of the algorithm model.

3. Results

In this section, three experiments are conducted to evaluate the recognition effectiveness, time performance, and robustness of the model.

3.1. Experiment 1: dividing training set and test set based on subject's numbers

In this experiment, the data of all subjects were randomly divided into two parts. Specifically, the 10 subjects were divided into a seven-person training set and a three-person test set. This means that the ratio of the training set to the test set is 7:3. The experimental setup based on subject's numbers is shown in Fig. 6. All the data included the subjects' gait data at three stride lengths and three speeds.

Based on the same IMU data of 10 subjects, we compared the cross-subject recognition ability of above models. Table 1 shows the recognition results of three cross-subjects under the DAE-LSTM model. For the three subjects (subject 1, subject 2, subject 3), the average recognition accuracy of DAE-LSTM was 90.12 %, 91.08 % and 90.03 %, respectively. The recognition confusion matrix of three subjects (subject 1, subject 2, subject 3) under four models is shown in Fig. 7. For the three subjects (subject 1, subject 2, subject 3), the average recognition accuracy of RF was 89.4 %, 88.3 %, and 87.7 %, respectively. The average recognition accuracy of SVM was 87.6 %, 89.1 % and 88.3 %, respectively. The average recognition accuracy of KNN was 85.8 %, 88.1 % and 86.9 %, respectively. The average recognition accuracy of NN was 88.4 %, 89.6 % and 88.4 %, respectively. Obviously, all the recognition accuracy of the four models is less than 90 %. The results showed that the recognition accuracy of the three cross-subjects were higher than 90 %. Compared with RF, SVM, KNN and NN, the DAE-LSTM model has better cross-subject recognition performance.

3.2. Experiment 2: time potential analysis of DAE-LSTM model recognition based on cross-subject data

The amount of time it takes the algorithm to reach a classification decision after receiving new data is the metric we are interested in. Specifically, the amount of time includes three parts: data acquisition time, filtering time and model recognition time. The time required for the first two parts is the same for different models. Therefore, the time

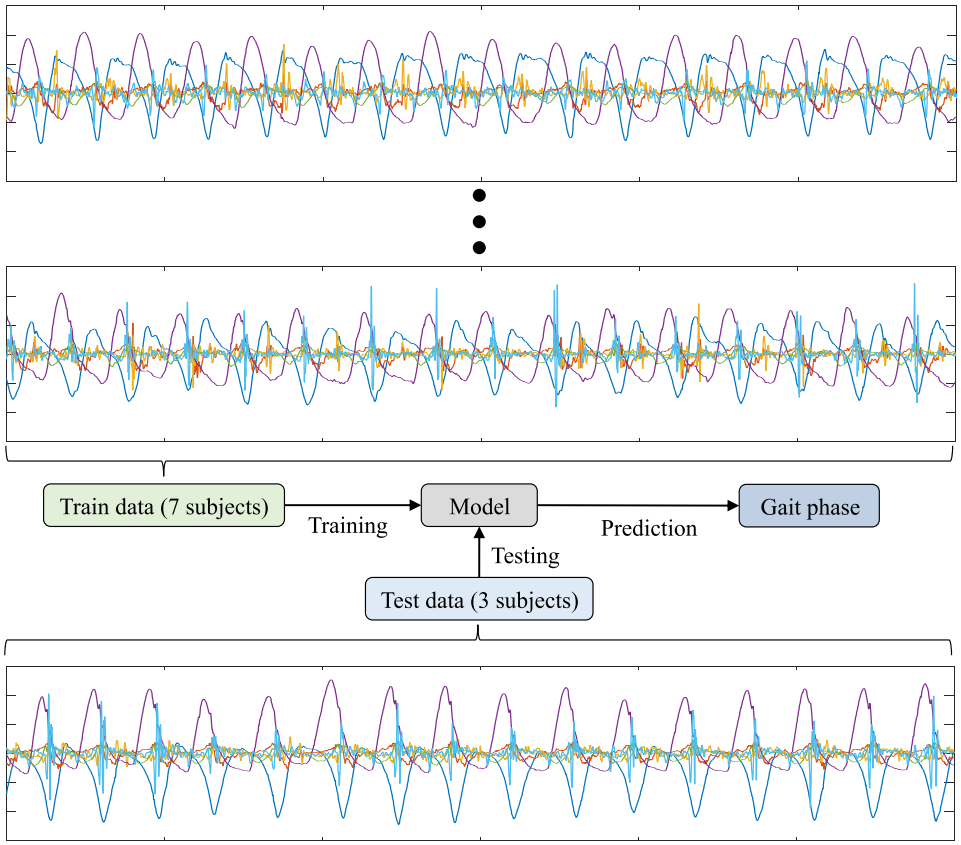

Fig. 6. Experimental setup instructions based on subject's numbers.

Table 1
Cross-subject confusion matrix based on DAE-LSTM (%).

		NDS	GFS	WDS	FTLS	
		Predict class				
S1	NDS	78.58	11.99	0	9.43	***Actual class***
	GFS	1.97	88.78	9.25	0	
	WDS	0	0	94.84	5.16	
	FLS	1.07	0.05	1.12	97.76	
	Total	**90.12**				
S2	NDS	84.46	6.36	0	9.18	
	GFS	2.22	92.47	5.25	0.06	
	WDS	0	1.12	87.20	11.68	
	FLS	1.63	0.03	0.25	98.09	
	Total	**91.08**				
S3	NDS	78.75	12.57	0	8.68	
	GFS	2.36	90.78	6.82	0.04	
	WDS	0.06	0.58	93.90	5.46	
	FLS	3.46	0	0.50	96.04	
	Total	**90.03**				

required for model recognition is the core element. We feed the filtered IMU data of cross-subject into DAE-LSTM model and record the recognition time.

In order to measure the recognition time of the DAE-LSTM model across the subject data, we program the time when recognition starts and the time when recognition ends. The total recognition time is obtained by the time between the recognition ending and recognition starting. The ratio of the total recognition time and total amount of data across the subject group is the average recognition time required per frame of data. For the above data, the experimental results showed that the total recognition time and total data volume were 15716.8 ms and 41015 frames, respectively.

Obviously, the average recognition time required per frame of data is 0.383 ms. It can be seen that the model shows good temporal performance for the filtered IMU data of cross-subject.

3.3. Experiment 3: robustness comparison of models based on data of different signal-to-noise ratios

Comparative experiments showed that the proposed method had good robustness under different SNR data. In this experiment, the division method of training set and test set was the same as in experiment 2.

In the test set, we artificially added different proportions of Gaussian white noise to the original signal. Then the data after adding noise are fed into different algorithm models and identified offline. The signal-to-noise ratio settings are 100:0.1, 100:0.25, 100:0.5, 100:1, 100:2.5, 100:5, 100:10, and 100:20, respectively. For different signals, we conducted ablation experiments and compared the recognition performance of the six models respectively.

The recognition results of the models are shown in Fig. 8. For signals without Gaussian white noise, the real-time recognition accuracy of DAE-LSTM and LSTM models is 90.2 %. The average accuracy of offline recognition of the other four models were 81.7 % (RF), 83.6 % (SVM), 83.8 % (KNN), and 84.5 % (NN), respectively. For signals with Gaussian white noise, the average offline recognition accuracy of the proposed DAE-LSTM model was 90.2 % (100:0.1), 90.2 % (100:0.25), 90.0 % (100:0.5), 90.0 % (100:1), 89.3 % (100:2.5), 88.2 % (100:5), 85.1 % (100:10), and 80.1 % (100:20), respectively. Corresponding to the signal-to-noise ratio of 100:0.1, 100:0.25, 100:0.5, 100:1, 100:2.5, 100:5, 100:10, and 100:20, the average accuracy of offline recognition of the LSTM model were 90.1, 90.1, 90.0, 89.4, 88.3, 86.4, 82.5, and 76.8 %, respectively. The average accuracy of offline recognition of NN

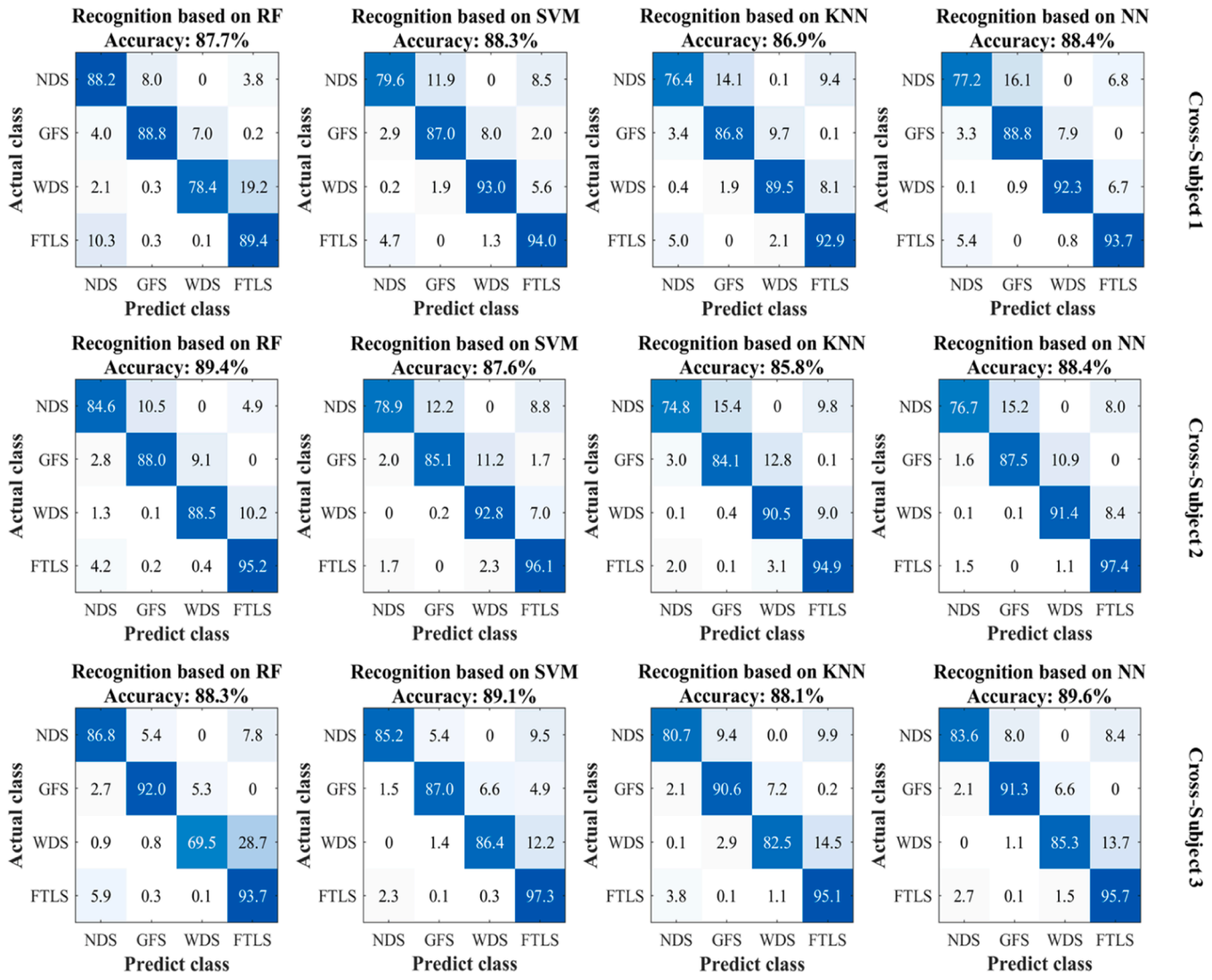

Fig. 7. The cross-subject recognition accuracy of the three subjects (subject1, subject2 and subject3) based on RF, SVM, KNN and NN models is determined.

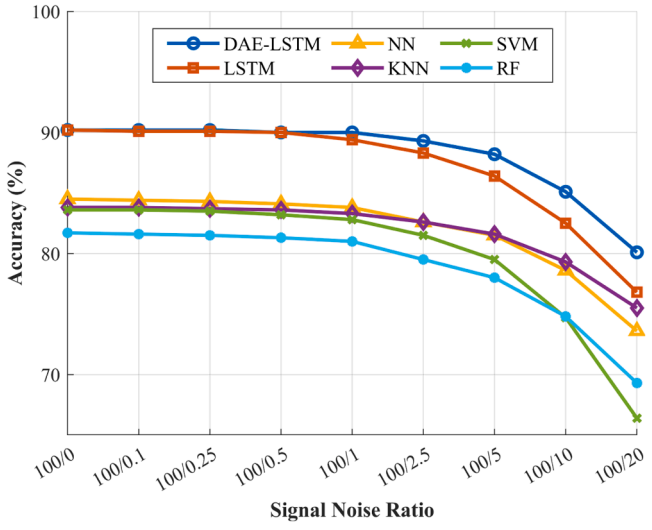

Fig. 8. Recognition results of 6 models with different SNR.

model were 84.4, 84.3, 84.1, 83.8, 82.6, 81.5, 78.6, and 73.6 %, respectively.The average accuracy of offline recognition of KNN model were 83.8, 83.7, 83.6, 83.3, 82.6, 81.6, 79.3, and 75.5 %, respectively. The average accuracy of offline recognition of SVM models were 83.6, 83.5, 83.2, 82.8, 81.5, 79.5, 74.7, and 66.4 %, respectively. The average accuracy of offline recognition of RF models were 81.6, 81.5, 81.3, 81.0, 79.5, 78.0, 74.8, and 69.3 %, respectively. When the signal-to-noise ratio was greater than 100:1, the accuracy of the DAE-LSTM model was higher than 90.0 %, and the accuracy of the other four models were less than 85 %. Obviously, the proposed DAE-LSTM was more robust than other models.

4. Discussion

4.1. Recognition accuracy and model recognition time

This paper proposed a DAE-LSTM recognition algorithm for lateral walking gait recognition. Compared to the RF, SVM, KNN and NN, the average recognition accuracy of the proposed method for the four gait phases (NDS, GFS, WDS and FLS) in cross-subject condition is the highest. In order to compare the recognition performance of the five models more intuitively, we plotted the recognition results of three cross-subjects under different models into a histogram as shown in Fig. 9. For the collected IMU signals, the cross-subject recognition results

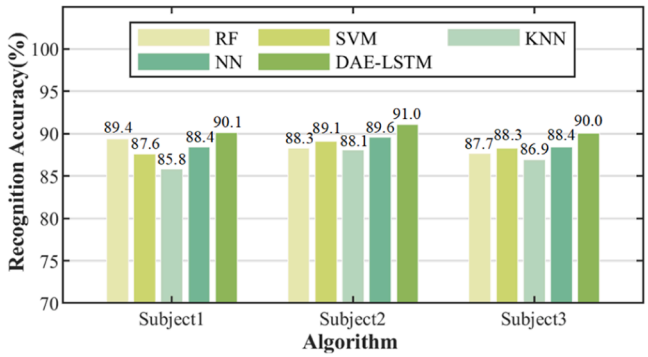

Fig. 9. Cross-subject recognition accuracy based on Five models.

of DAE-LSTM were 90.12 % (subject 1), 91.08 % (subject 2), and 90.03 % (subject 3). The other models achieved cross-subject recognition results below 90 %. Among them, NN showed better recognition effect than RF, SVM and KNN, 88.4 % (subject 1), 89.6 % (subject 2) and 88.4 % (subject 3), respectively. The DAE-LSTM model showed stronger cross-subject recognition ability. The reason may be that the LSTM module had ability to extract features, while traditional classification models relied more on manual feature extraction and resulting in loss of some features [24]. Liu et al. used LSTM to identify the four gait types based on the sEMG signal and achieved high recognition accuracy [25]. The method proposed in this study can reach a high technical level in cross-subject recognition results. It can provide a good reference for the future development of this field.

In this study, the IMU signals acquisition frequency is 200 Hz. In other words, the sampling interval between each frame of data is 5 ms. Real-time recognition requires signal processing and model recognition of the previous frame of data within the sampling interval. The results show that the average recognition time of DAE-LSTM for each frame of data is much less than 5 ms. This means that the algorithm can recognize the corresponding gait phase of the frame data by 0.383 ms after receiving the new data. This new data can be either within the same phase or transitional data between adjacent phases. Therefore, the proposed algorithm has the potential of real-time recognition.

4.2. Model robustness

We artificially added different proportions of white Gaussian noise to the cross-subject group signals [26]. The selected SNR values range from 100:0.1–100:20. This is to simulate a variety of real-world scenarios, from high quality data to strong noise data, in order to comprehensively evaluate the robustness of the algorithm. These SNR values cover the noise range from very small to very large, and are consistent with the noise levels that IMU signals may be subjected to in practical applications. Then, experiments are performed in offline mode (The process of evaluating the input of pre-recorded test set data containing noise into the model.) to conduct robust analysis of the model. As can be seen from Fig. 8, the average recognition accuracy of the model decreases with the increase of noise. The proposed DAE-LSTM model still maintains a recognition accuracy of 90.0 % when the SNR value is 100:1, while the accuracy of the other five models is lower than 90 %. With the increase of noise, when SNR is 100:20, the accuracy of DAE-LSTM model is 80.1 %, while that of other models is 76.8 % (LSTM), 73.6 % (NN), 75.5 % (KNN), 66.4 % (SVM) and 69.3 % (RF), respectively. To evaluate the performance of the DAE-LSTM model versus a separate LSTM model, an ablation experiment was performed. As can be seen from Fig. 8, when the SNR is greater than 100:1, there is little difference in recognition accuracy between the two models. This is because less noise is added and the effect on the original signal is not obvious. When the SNR is less than 100:1, the difference in recognition accuracy between the two models becomes greater. When adding more noise, the trained DAE can reconstruct signals similar to the original signals to a certain extent. Compared with the single LSTM model, the DAE-LSTM model has the ability to reconstruct noise, so it has more advantages in recognizing signals containing certain noise. To make the results more convincing, we added the paired T-test results to prove that the robustness of DAE-LSTM is significantly better than other models. Specifically, we performed a paired T-test for accuracy results across all noise levels (SNR Settings) to assess the significance of performance differences between DAE-LSTM and other models. Through calculation, the P value of DAE-LSTM and LSTM is 0.021, and the P value of DAE-LSTM and other four models is about 0.00001. The results showed that the accuracy of DAE-LSTM compared with other models at all SNR levels was statistically significant ($P < 0.05$). To sum up, for signals with different SNR settings, the offline recognition accuracy of the proposed DAE-LSTM model is higher than that of the other four models, and it has better robustness.

4.3. Performance comparison

As far as we know, the research on lateral walking gait recognition is almost blank. The first current research in this field is our previous work [9]. However, our previous work only identified lateral walking gaits with fixed stride length. It is considered that there are some differences in the lateral stride length and speed of different people. In this study, we explored the identification of lateral walking gaits at three stride lengths and three speeds. As shown in Fig. 10(a), the previous work used a traditional model. The average cross-subject recognition accuracy of the model is 89.63 % on the data with fixed strid e length and three speeds. On the basis of previous studies, the gait recognition algorithm is optimized and improved according to the time characteristics of data. Under three stride lengths and three speeds, the average cross-subject recognition accuracy of the DAE-LSTM model reaches 90.41 %, which provides better recognition performance support for the development of lateral walking gait recognition.

As shown in Fig. 10(b), we also compare the model recognition time of this study with that of previous work. We can see that the previous model had an average recognition time of 5.7 ms per frame of data. On the basis of previous studies, the average recognition time of each frame of data by the DAE-LSTM model in this study can reach 0.38 ms. Compared with the previous work, the time performance of the model is improved by 5.32 ms. This has great significance for the real time requirement of exoskeleton. The reason for this may be that the previous model was a simple machine learning algorithm similar to KNN. The output is predicted mainly based on the new data's nearest neighbors in the training set. For time series data, KNN typically converts the data into a fixed-size window and queries each new sample with its nearest training sample. The recognition time depends mainly on the size and number of data points, and the number of neighbors (K value). In general, the recognition time of KNN is proportional to the size of the training data set because each new sample needs to be searched and computed. The DAE-LSTM in this study is a complex deep learning model, which is particularly suitable for processing and predicting series-dependent problems in time series data. DAE-LSTM predicts future values of time series by learning long-term dependencies. Even if the amount of data is large, as long as the model has adapted to the data pattern during the training phase, the time to predict a single sample is usually not too long, especially for the model that has already been trained.

Forward walking and lateral walking are similar in many basic biomechanical properties, but there are also significant differences. In terms of gait phase and gait periodicity, both forward walking and lateral walking contain basic gait phases, such as support phase and swing phase. In addition, both exhibit a cyclical movement pattern in which walking is completed through repetitive movements of the lower limbs. In terms of movement direction and application scenarios, forward walking is mainly to move in the front and back direction of the

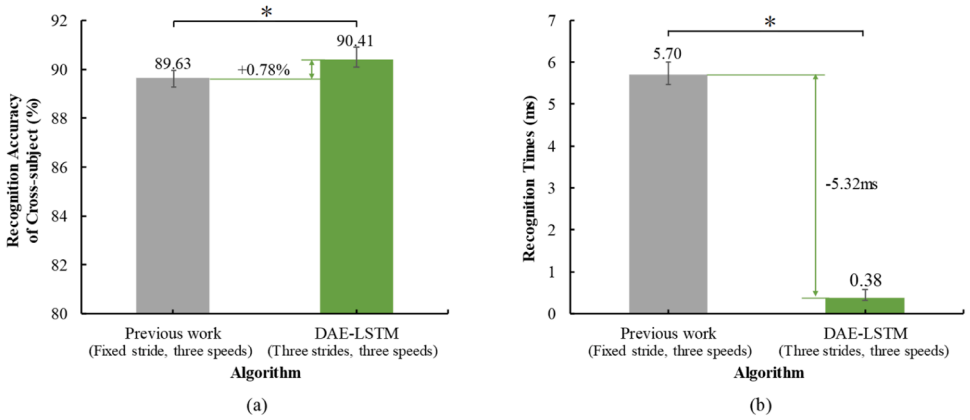

Fig. 10. Performance comparison between DAE-LSTM (Three strides and three speeds) and previous work (Fixed stride and three speeds). (a) Comparison of cross-subject recognition accuracy between previous work and DAE-LSTM. (b) Comparison of model recognition time between previous work and DAE-LSTM.

body, which is a common way of daily walking. Lateral walking, however, is mainly a lateral movement along the body, with more emphasis on horizontal balance, and is usually used in specific scenarios such as rehabilitation training or sports training. In terms of muscle activation, forward walking has significant activation effect on hip flexor extensor muscle. Lateral walking relies more on the activation of the hip abductor muscle to control lateral stability.

We also analyze and discuss the results of lateral walking gait recognition based on IMU signal and the latest results of forward walking gait recognition. Guo et al. proposed an automatic and robust recognition method for gait phases across multiple walks and different walking speeds based on temporal convolutional networks (TCN). Cross-subject experiments were carried out by walking on the ground and walking on a treadmill, and the accuracy of recognition was 0.7693 $\pm$ 0.082 and 0.7607 $\pm$ 0.078, respectively [31]. Mohamed et al. propose a hybrid approach to establish a posterior belief by combining prior biomechanical signal knowledge, heuristics, and pattern recognition, using kinematic feedback from four inertial measurement units (IMUs) to form an open source dataset for validation and benchbreaking of short-long-term memory (LSTM) models. Experimental results show that the average online accuracy of invisible objects is 97.94 % [32]. From the above latest research results on forward gait recognition, we can see that there are relatively mature research results on forward gait recognition, and they show high accuracy and model performance, indicating that the deep learning method based on IMU data has high potential. As a relatively new research field, the difficulty of transverse gait recognition is mainly due to its special motion direction, gait phase characteristics and less research basis. This indicates that the research results of forward gait recognition can provide valuable reference and methodology support for lateral gait recognition in the future.

In addition to IMU-based gait recognition, we acknowledge that vision-based gait recognition has gained significant attention in recent years. For example, Wang et al. proposed a novel event-based gait recognition method, which uses two different representations of event streams: graph-based and image-based. These representations are processed by Graph Convolutional Networks (GCN) and Convolutional Neural Networks (CNN) for gait recognition. The methods, named EV-Gait-3DGraph and EV-Gait-IMG, show that EV-Gait-3DGraph achieves significantly higher recognition accuracy compared to other competing methods when sufficient training samples are available [33]. Gu et al. mapped noisy data from RGBD and wearable sensors to precise 4D representations of the lower limbs and joints, obtained from an accurate motion capture (Mocap) system. They proposed a series of deep architectures that encode cross-modal and cross-subject transfer for abnormal gait recognition [34]. Zhao et al. used an embedded robotic camera to capture leg motion data and conducted comparative tests and error analysis to accurately describe gait patterns. They introduced a new ESMF algorithm to precisely assess turn angles, effectively addressing the issue of missing landmark points and recognizing drag gait and falls [35]. Hu et al. proposed a novel Graph Convolutional Neural Network (GCNN) architecture, where each video is represented as a directed graph, with the FoG-related candidate regions as vertices, rather than learning the overall video representation. They also introduced a weakly supervised learning strategy and a weighted adjacency matrix estimation layer to reduce the expensive data annotation required for fully supervised learning. By identifying vertices that lead to FoG events, they improved FoG detection performance [36]. In contrast, IMU-based gait recognition offers significant advantages in terms of portability, robustness, and usability for real-world applications like wearable exoskeletons. IMUs are less affected by environmental factors and can provide continuous gait recognition with minimal computational overhead. In future work, we plan to explore multi-modal approaches that combine visual and IMU data to improve gait phase recognition accuracy. This could provide a more comprehensive solution for exoskeleton control and rehabilitation applications.

4.4. Limitation

The proposed DAE-LSTM model achieves good recognition accuracy and strong robustness. However, it has certain limitations. Although the dataset includes lateral gait data with asynchronous stride length and speed, there is still room for improvement in dataset size and subject diversity. In the future, we will expand the dataset by including more subjects with different genders, ages, and body types. Additionally, further algorithmic refinements will be made to enhance robustness and applicability. The Kalman filter used in this study effectively optimizes IMU signals. However, the filtering process inevitably leads to the loss of some signal details. To address this, we plan to explore alternative filtering methods to minimize signal loss in future work. While the model demonstrates good overall recognition accuracy across subjects, its accuracy in recognizing specific gait phases requires further improvement. Stride length and hip range of motion during lateral walking may also affect gait recognition accuracy and the efficiency of exoskeleton control. Finally, this study evaluates the model's performance in an offline setting. In future work, we plan to deploy the model in an exoskeleton system and optimize it for real-time validation in real-world scenarios.

5. Conclusion

In this study, we used the IMUs to collect the attitude information of lateral walking gait. Given the time-dependent performance of lateral gait and the perturbed characteristics of IMU signals, we proposed the first algorithm for lateral walking gait recognition (DAE-LSTM). The

lateral walking gait phases at three speeds and three strides were identified. Compared to RF, SVM, KNN and NN, the proposed method can achieve the requirements of recognition accuracy, model recognition time and model robustness at the same time. This study provides a preliminary exploration of lateral walking gait recognition and can be applied to a team-designed exoskeleton for lateral resistance walk exercise. In future work, we plan to embed the method proposed in this paper into the exoskeleton system for lateral resistance walking training, collect the user's IMU data in real time, identify the gait phase in real time through the algorithm, and transmit the recognition results to the exoskeleton controller to control the corresponding speed and torque output by the motor, so as to achieve accurate control and synchronization of the exoskeleton. Future exoskeleton tests will further verify the performance of the algorithm in terms of real-time, control accuracy and stability.In addition, we plan to explore the application of the algorithm in other lateral motion modes, such as gait analysis in athlete training and gait monitoring in assistive devices for the elderly. This will further verify the generality and practical value of the proposed method.

Author statement

Mingxiang Luo: Conceived the research idea, designed the experiments, and wrote the main draft of the manuscript. Xiaoli Dong: Assisted in data collection, experimental setup, preprocessing of IMU signals, and participated in the creation of some figures. Hongliu Yu: Supervised the research project, performed grammar and logical revisions of the manuscript. Mingming Zhang: Provided domain expertise in gait analysis, performed grammar and logical revisions of the manuscript. Xinyu Wu: Supervised the research project, guided methodological improvements, secured funding and performed critical technical and academic revisions of the manuscript. Worawarit Kobsiriphat: Conducted the literature review, and wrote the discussion on related work. Jing-Xin Wang: Contributed to writing and grammar corrections of the manuscript. Wujing Cao: Oversaw the overall planning and execution of the research, secured funding, and provided final approval for the submission of the manuscript.

CRediT authorship contribution statement

Mingxiang Luo: Writing – original draft. **Mingming Zhang**: Formal analysis. **Xinyu Wu**: Methodology. **Xiaoli Dong**: Data curation. **Hongliu Yu**: Conceptualization. **Wujing Cao**: Writing – review & editing, Funding acquisition. **Worawarit Kobsiriphat**: Investigation. **Jing-Xin Wang**: Project administration.

Declaration of Competing Interest

The authors declare that they have no known competing financial interests or personal relationships that could have appeared to influence the work reported in this paper.

Acknowledgments

This work was supported in part by the Shenzhen Science and Technology Program (JCYJ20220531100808018, RCBS20210706092252054), in part by the National Natural Science Foundation of China under Grant 62003327, in part by the Guangdong Basic and Applied Basic Research Foundation under grant 2024A1515030055, and in part by the Shenzhen Institute of Artificial Intelligence and Robotics for Society.

References

[1] Willcox EL, Burden AM. The influence of varying hip angle and pelvis position on muscle recruitment patterns of the hip abductor muscles during the clam exercise. J Orthop Sports Phys Ther 2013;33(5):325–31.
[2] Distefano LJ, Blackburn JT, Marshall SW, Padua DA. Gluteal muscle activation during common therapeutic exercises. J Orthop Sports Phys Ther 2009;39(7):532–40.
[3] Morbidoni C, Cucchiarelli A, Agostini V, Knaflitz M, Fioretti S, Di Nardo F. Machine-learning-based prediction of gait events from EMG in cerebral palsy children. IEEE Trans Neural Syst Rehabil Eng 2021;29:819–30 (May).
[4] Wei P, Zhang J, Tian F, Hong J. A comparison of neural networks algorithms for EEG and sEMG features based gait phases recognition. Biomed Signal Process Control 2021;68:1746–8094.
[5] Cheng S, Bolívar-Nieto E, Gregg RD. Real-time activity recognition with instantaneous characteristic features of thigh kinematics. IEEE Trans Neural Syst Rehabil Eng 2020;29:1827–37.
[6] Bartlett HL, Goldfarb M. A phase variable approach for IMU-based locomotion activity recognition. IEEE Trans Neural Syst Rehabil Eng 2018;65(6):1330–8.
[7] Su B-Y, Wang J, Liu S-Q, Sheng M, Jiang J, Xiang K. A CNN-based method for intent recognition using inertial measurement units and intelligent lower limb prosthesis. IEEE Trans Neural Syst Rehabil Eng 2019;27(5):1032–42.
[8] Chen X, Zhang K, Liu H, Leng Y, Fu C. A probability distribution model-based approach for foot placement prediction in the early swing phase with a wearable IMU sensor. IEEE Trans Neural Syst Rehabil Eng 2021;29:2595–604.
[9] Yang L, Xiang K, Pang M, Yin M, Wu X, Cao W. Inertial sensing for lateral walking gait detection and application in lateral resistance exoskeleton. IEEE Trans Instrum Meas 2023;72:1–14 (Art).
[10] Stolyarov R, Burnett G, Herr H. Translational motion tracking of leg joints for enhanced prediction of walking tasks. IEEE Trans Biomed Eng 2018;65(4):763–9.
[11] Ryu J.-H., Kim D.-H., "Multiple gait phase recognition using boosted classifiers based on sEMG signal and classification matrix," In Proceedings of the 8th International Conference on Ubiquitous Information Management and Communication (ICUIMC '14), Jan; 2014.
[12] Bruinsma J, Carloni R. IMU-based deep neural networks: prediction of locomotor and transition intentions of an osseointegrated transfemoral amputee. IEEE Trans Neural Syst Rehabil Eng 2021;29:1079–88.
[13] Wei B, Ding Z, Yi C, Guo H, Wang Z, Zhu J, Jiang F. A novel sEMG-based gait phase-kinematics-coupled predictor and its interaction with exoskeletons. Front Neurorobotics 2021:107 (Aug).
[14] Luo R, Sun S, Zhang X, Tang Z, Wang W. A low-cost end-to-end semg-based gait sub-phase reco gnition system. IEEE Trans Neural Syst Rehabil Eng 2020;28(1):267–76.
[15] Jun K, Lee D-W, Lee K, Lee S, Kim MS. Feature extraction using an rnn autoencoder for skeleton-based abnormal gait recognition. IEEE Access 2020;8:19196–207.
[16] Tu J., Liu H., Meng F., Liu M., Ding R., Spatial-temporal data augmentation based on LSTM autoencoder network for skeleton-based human action recognition," Processings of the 25th IEEE International Conference on Image Process;2018; p. 3478-3482.
[17] Zhang Z, Tran L, Liu F, Liu X. On learning disentangled representations for gait recognition. 1 Jan IEEE Trans Pattern Anal Mach Intell 2022;44(1):345–60. 1 Jan.
[18] Sheng W, Li X. Siamese denoising autoencoders for joints trajectories reconstruction and robust gait recognition. Neurocomputing 2020;395:86–94.
[19] Wang Q, Ye L, Luo H, Men A, Zhao F, Huang Y. Pedestrian stride-length estimation based on LSTM and |oencoders. Sensors 2019;19(4):840.
[20] Zou Q, Wang Y, Wang Q, Zhao Y, Li Q. Deep learning-based gait recognition using smartphones in the wild. IEEE Trans Inf Forensics Secur 2020;15:3197–212.
[21] Wu X, Yuan Y, Zhang X, Wang C, Xu T, Tao D. Gait phase classification for a lower limb exoskeleton system based on a graph convolutional network model. IEEE Trans Ind Electron 2022;69(5):4999–5008.
[22] Liu J, Zhou X, He B, Li P, Wang C, Wu X. A novel method for detecting misclassifications of the locomotion mode in lower-limb exoskeleton robot control. IEEE Robot Autom Lett 2022;7(3):7779–85.
[23] Wu Y., Zheng B., Zhao Y., Dynamic gesture recognition based on LSTM-CNN," Proceedings of the China Automation Congress. (CAC); 2018. p. 2446-2450, Nov./Dec.
[24] Park K.-H., Lee S.-W., "Movement intention decoding based on deep learning for multiuser myoelectric interfaces," Proceedings of the 4th International Winter Conference on Brain-Computer Interface; 2016; p. 1–2.
[25] Liu J, Wang C, He B, Li P, Wu X. Metric learning for robust gait phase recognition for a lower limb exoskeleton robot based on sEMG. IEEE Trans Med Robot Bionics 2022;4(2):472–9.
[26] Xu D, Wang Q. On-board Training Strategy for IMU-Based Real-Time Locomotion Recognition of Transtibial Amputees With Robotic Prostheses. Front neurorobotics 2020;14:47.
[27] Rokhmanova N, Pearl O, Kuchenbecker KJ, Halilaj E. IMU-based kinematics estimation accuracy affects gait retraining using vibrotactile cues. IEEE Trans Neural Syst Rehabil Eng 2024;32:1005–12.
[28] Guo Z, Wu H, Fang J, Zhang J, Long J. Online transfer learning with pseudo label for gait phase prediction. IEEE Trans Instrum Meas 2024;73:1–15.
[29] Chen W, Li C, Fang X, Zhang Q. A method for real-time prediction of gait events based on walking speed estimation. IEEE Sens J 2024;24(22):37986–96. 15 Nov.15.
[30] Liu Y, Liu Y, Song Q, Wu D, Jin D. Gait event detection based on fuzzy logic model by using IMU signals of lower limbs. IEEE Sens J 2024;24(14):22685–97. 15 July15.
[31] Guo Y, Hutabarat Y, Owaki D, Hayashibe M. Speed-variable gait phase estimation during ambulation via temporal convolutional network. IEEE Sens J 2024;24(4):5224–36. 15 Feb.15.

[32] Mohamed S.A., Martinez-Hernandez U., A Hybrid Bayesian-Heuristic Inference System for Recognition of Gait Phase, International Joint Conference on Neural Networks (IJCNN), Yokohama, Japan; 2024.
[33] Wang Y, Zhang X, Shen Y, Du B, Zhao G, Cui L, Wen H. Event-stream representation for human gaits identification using deep neural networks. IEEE Trans Pattern Anal Mach Intell 2022;44(7):3436–49.
[34] Gu X, Guo Y, Deligianni F, Lo B, Yang G-Z. Cross-subject and cross-modal transfer for generalized abnormal gait pattern recognition. IEEE Trans Neural Netw Learn Syst 2021;32(2):546–60.
[35] Zhao D, Yang J, Okoye MO, Wang S. Walking assist robot: a novel non-contact abnormal gait recognition approach based on extended set membership filter. IEEE Access 2019;7:76741–53.
[36] Hu K, Wang Z, Mei S, Martens KA Ehgoetz, Yang T, Lewis SJG, Feng DDagan. Vision-based freezing of gait detection with anatomic directed graph representation. IEEE J Biomed Health Inform 2020;24(4):1215–25.